Research Paper   **Engineering**

Bainitic Transformation During Austempering of Ductile Cast Iron

Zdzisław Ławrynowicz

University of Science and Technology UTP, Mechanical Engineering Faculty, Department of Materials Science and Engineering, av. Kaliskiego 7, 85-796 Bydgoszcz, Poland, E-mail: lawry@utp.edu.pl

ABSTRACT

The investigation was carried out to examine the influence of temperature and times of austempering on the extent of bainite reaction and carbon content in retained austenite. The comparison of experimental data with the T_0, T_0' and A_{e3}' phase boundaries suggests the likely mechanism of bainite reaction in cast iron is displacive rather than diffusional. Experimental measurements of volume fraction of bainitic ferrite and carbon diffusion distance in austenite indicate that there is a necessity of carbides precipitation. A consequence of the precipitation of cementite from austenite during austempering is that the growth of bainitic ferrite can continue to larger extent and that the resulting microstructure is not an ausferrite but is a mixture of bainitic ferrite, retained austenite and carbides.

KEYWORDS   Ausferrite, Bainite, Ductile cast iron ADI, Decarburisation, Carbon diffusion distances

1. INTRODUCTION

The development of austempered ductile iron (ADI) is a major achievement in cast iron technology. The starting material for the development of ADI is the high quality ductile or nodular cast iron. It is then subjected to an isothermal heat treatment process known as "austempering". The attractive properties of ADI are related to its unique microstructure that consists of ferrite and high carbon austenite. Because of this microstructure, the product of austempering reaction in ductile iron is often referred to as "ausferrite" rather than bainite.[1,2,3] Once the ausferrite has been produced, the components are cooled to room temperature. The cooling rate will not affect the final microstructure as the carbon content of the austenite is high enough to lower the martensite start temperature to a temperature significantly below room temperature. If ADI is held for long time periods, the high carbon austenite will eventually undergo a transformation to bainite, the two phase mixture of ferrite and carbide ($\alpha + Fe_3C$). In order for this transformation to occur, longer periods of time are typically needed – much longer than would be economically feasible for the production of ADI.

Fig. 1 shows a schematic of the austempering process that includes two major steps: austenitising and isothermal heat treatment at the austempering temperature.
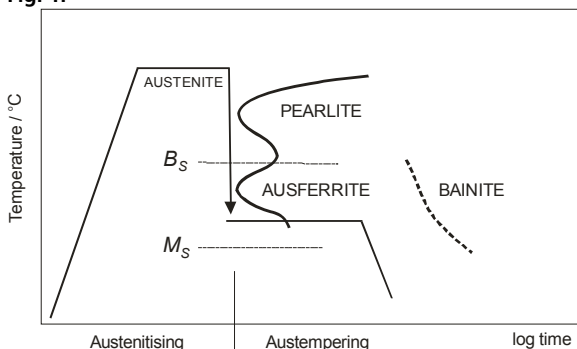
Fig. 1.

Fig. 1. Schematic of the austempering process [3]

Also graphite nodule count in ductile iron to be austempered and its uniform distribution can influence on carbon diffusion distance. Low nodule counts lead to larger spacing between the graphite nodules and larger regions of segregation. In the worst case scenario, these regions can become so heavily segregated that they do not fully transform during austempering, resulting in the formation of low carbon austenite or even martensite. Higher nodule counts will break up the segregated regions.

The austempering heat treatment enables the ductile cast iron containing mainly strong bainitic ferrite and ductile carbon-enriched austenite, with some martensite transforms from austenite during cooling down to room temperature.[4,5]

Fully bainitic austempered ductile irons are free from allotriomorphic ferrite and almost free from athermal martensite. The structure is thus composed of retained austenite, bainitic ferrite and carbides (Fig. 2). Carbides however, can be suppressed by alloying with elements such as Si and Al. Large amount of silicon present in ductile iron suppresses the precipitation of carbide during austempering reaction and retains substantial amount of stable high carbon austenite. The formation of carbides is undesirable, especially if a component is to be machined after heat treatment. Thus, the toughness of an ADI component can be severely compromised by the presence of non-metallic inclusions and carbides even if their levels were acceptable for conventional ductile iron.
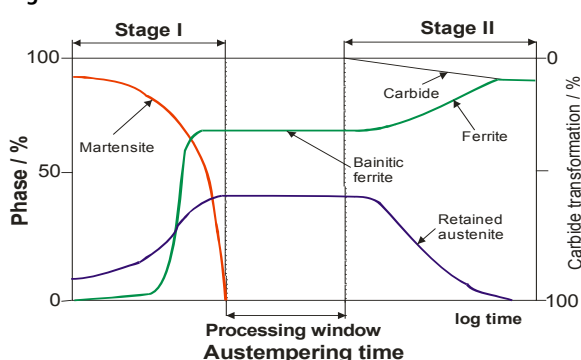
Fig. 2.

Fig. 2. Schematic representation of the development of microstructure during austempering, together with an illustration of the 'processing window'. Martensite is present only when the sample is cooled to room temperature before the austempering has been completed [4,5]

Cast iron usually contains about 2 wt.% or more of silicon, which is well known to retard the formation of cementite.[4] The bainite in ADI therefore contains no cementite in austenite, which is then enriched with carbon and can be retained as austenite at ambient temperature. A key factor controlling the stability of the retained austenite is its carbon concentration therefore the ductile iron should be held at austenitising and austempering temperatures and for a time sufficient to create an austenite matrix that is saturated with carbon.

The purpose of the present paper is to demonstrate how a thermodynamic method can be used for solving a problem of the decarburisation of bainite laths and carbon diffusion distances in the matrix of ADI. This should in principle enable to examine the possibility of carbides precipitation in ADI.

2. MATERIAL AND METHODS

The chemical composition of the experimental ductile iron is listed in Table 1. The concentration of alloying elements in the matrix is obtained from the chemical analysis. Ductile iron blocks were produced in a commercial foundry furnace. The melt was poured into a standard Y block sands molds (ASTM A-395), which ensured sound castings. Specimens austenitised at T_γ = 950 and 830°C for 60 minutes were rapidly transferred to a salt bath at austempering temperatures 250, 300, 350 and 400°C, held for 15, 30, 60, 120 and 240 minutes and then water quenched to room temperature. The microstructure of the as-cast material matrix contains 40% ferrite and 60% pearlite, however graphite nodules in material is 11.5%.

After heat treatment, the samples were prepared for metallographic analysis. The samples were etched using 2% nital. Optical micrographs were taken with a Nikon camera attached to a light microscope. The two-stage carbon replicas were examined using a TESLA BS 540 transmission electron microscope operated at 80 kV.

Table 1. Chemical composition of ductile cast iron ADI, wt-%

C	Si	Mn	P	S	Mg	Cr	Ni	Mo
3.21	2.57	0.28	0.06	0.01	0.024	0.036	0.098	0.015

The *X*-ray investigations were performed on the specimens heat treated after specific time of the isothermal bainite reaction at the given temperature. The total volume fraction of the retained austenite was measured from the integral intensity of the $(111)\gamma$ and $(011)\alpha$ peaks. The presence of high silicon content in ADI retards the formation of cementite in ferrite and austenite. The carbon concentration in retained austenite was calculated from measured lattice parameter of the retained austenite. The *2θ* values for austenite peaks were used to calculate the *d* spacing with Bragg's law and then the lattice parameters. The lattice parameter of austenite (a_γ) is related to the known relationship between the parameter and the carbon concentration[3]:

$$a_\gamma(nm) = 0.3573 + 0.0033\, x_\gamma \qquad (1)$$

where x_γ is the carbon concentration in austenite, in weight %. The matrix carbon concentration was also estimated analytical as[3]:

$$x_\gamma = -0.435 + (0.335 \times 10^{-3})\,T_\gamma + (1.61 \times 10^{-6})\,T_\gamma^2 + \qquad (2)$$
$$+ 0.006(\%Mn) - 0.11(\%Si) - 0.07(\%Ni) +$$
$$+ 0.014(\%Cu) - 0.3(\%Mo)$$

where x_γ is the estimated carbon concentration of the austenite at the austenitising temperature . T_γ .[3]

The measured matrix carbon concentration after direct quenching from austenitising temperature 950°C is x_γ =1.05%C and the calculated carbon content in matrix is x_γ' =1.044%C. After quenching from 830°C the calculated carbon content in matrix is x_γ =0.659%C and the measured

carbon content is x_γ =0.65%C, thus, the measured values were taken for further calculation.

3. RESULTS
3.1 Volume fraction of bainitic ferrite

The determined carbon concentrations of the residual austenite at the different stages of the formation of bainite (after austempering for 15, 30, 60, 120 and 240 minutes) are compared with the T_0, T_0' and Ae'_3 phase boundaries for investigated ADI in Figure 3. The diagram was calculated using a model developed by Bhadeshia[6] based on the McLellan and Dunn quasi-chemical thermodynamic model.[7] The martensite reaction starts temperature M_S is also marked on this diagram. The M_S temperature is a characteristic of the specific alloy composition and in particular the carbon concentration. The M_S is generally higher when the residual austenite has lower carbon content. The martensite M_S^* start temperatures was calculated using the method developed by Bhadeshia and it equals M_S = 117°C.[8]

In presented diagram the reaction is found to stop when the average carbon concentration of the residual austenite is closer to the T_0' curve than the Ae'_3 boundary. It is usually assumed that the point where the microstructure of austempered ADI ceases to change represents full transformation. But in case of bainitic transformation, reaction ceases before the parent phase (austenite) has completely transformed. It means that at any temperature below B_S and in the absence of any interfering secondary reactions only a limited quantity of bainitic ferrite forms before the reaction terminates. The presented results can be explained when it is assumed that bainitic ferrite grows without diffusion, but any excess of carbon is soon afterwards rejected into the residual austenite by diffusion.[9,10]
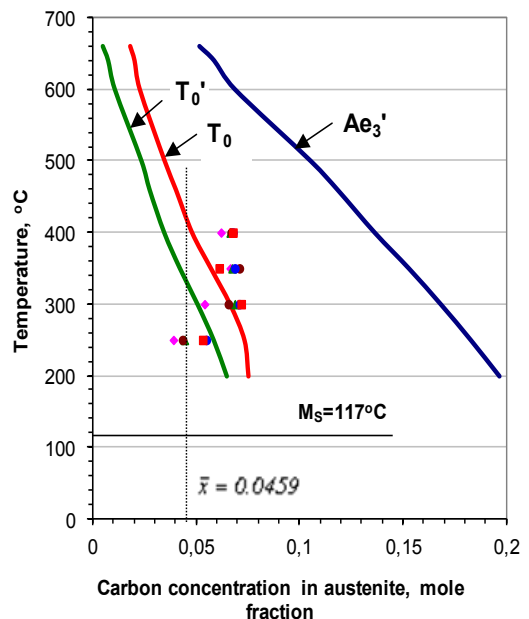
Fig. 3.

Fig. 3. The calculated phase boundaries T_0, T_0' and A_{e3}' for the investigated ADI together with all the experimental data of the measured carbon contents of the austenite

This makes more difficult for subsequent bainitic ferrite to grow, when the austenite becomes stabilised by increased carbon concentration. The maximum extent to which the bainite reaction can proceed is therefore determined by the composition of the residual austenite. A stage where diffusionless growth becomes thermodynamically impossible and the for-

mation of bainitic ferrite terminates is where the carbon concentration of the austenite reaches the T_0' or T_0 curves. Thus, the incomplete reaction phenomenon supports the hypothesis that the growth of bainitic ferrite occurs without any diffusion with carbon being partitioned subsequently into the residual austenite. If on the other hand, the ferrite grows with an equilibrium carbon concentration then the transformation should cease when the austenite carbon concentration reaches the Ae'_3 curve.[10-13]

Thus, it is found experimentally that the transformation to bainite does indeed stop close to the T_0 boundary. In Figure 3 the reaction seems to stop closer to the T_0 line than to the T_0' boundary. This might be explained by the fact that the T_0' line accounts for 400 J/mol of stored energy in the bainite. If this energy is reduced by plastic deformation of the surrounding austenite then a higher volume fraction of bainite should be able to form.

When the matrix of ADI only consists of ausferrite, thus:

$$V_\gamma + V_\alpha = 1 \qquad (3)$$

and the permitted fraction of bainite (V_α) can be determined from Lever rule applied to the T_0 curve, (Fig. 4).

The maximum volume fraction of retained austenite (V_γ) will then equal 1- V_α.

In case of carbides precipitation the maximum volume fraction of bainitic ferrite (V_α) can be calculated using the following equation[14]:

$$V_\alpha = \frac{x_{To} - \bar{x}}{x_{To} - x_\alpha - x_C} \qquad (4)$$

where V_α is volume fraction of bainitic ferrite, $\bar{x}$ is the average carbon concentration in the alloy, x_α is the paraequilibrium carbon concentration in the bainitic ferrite (0.03 wt. %), x_{To} is the carbon concentration of the austenite corresponding to the T_0 curve, x_C is the amount of carbon, which is tied up as carbides (cementite).
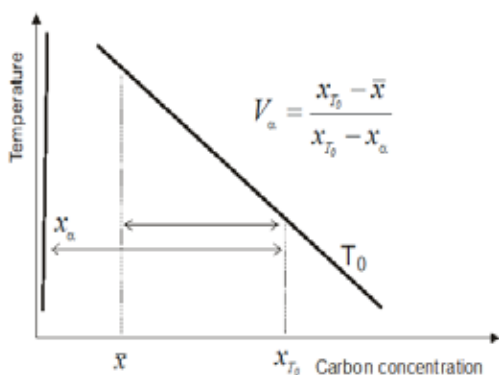
Fig. 4.

Fig. 4. Application of the Lever-rule to the To curve allows the estimation of the permitted fraction of bainite (Vα at any temperature (where for 950ºC =1.05 wt.% C, xα= 0.03%C).

Thus, the maximum volume fraction of bainite taking into account cementite precipitation can be calculated using the relationship (4).

It is seen in Fig. 5 that precipitation of cementite leads to an increase of volume fraction of bainitic ferrite. Carbides locally reduce the carbon content of the parent austenite and increase the driving force for further ferrite growth. The measured volume fraction of bainite is also shown in Fig. 5. Comparison of the calculated and measured fractions of bainite indicate that during bainite transformation in ADI must be intensive cementite precipitation.
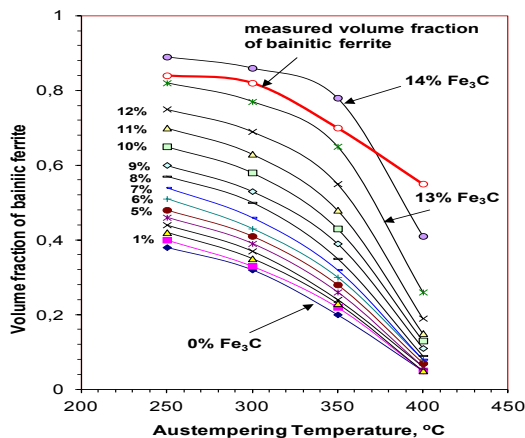
Fig. 5.

Fig. 5. Measured and calculated the maximum volume fraction of bainite in investigated ADI taking into account cementite precipitation in the range from 0% to 14% Fe_3C
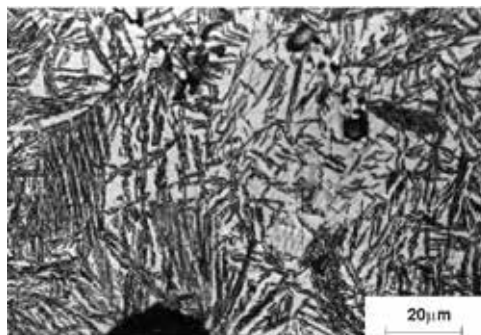
3.2. Microstructure
General features of the microstructure at the cell boundaries illustrated in Figs. 6 and 7 show how the morphology of bainitic ferrite changes with austempering temperature. The thermodynamic restriction imposed by the T_0 curve on the extent of bainite transformation can result in the formation of pools of retained austenite with a coarse, blocky morphology (Fig. 6b). As the austempering temperature increases the sheaves of bainite become thicker and so the laths are easier to resolve (Fig. 6). However, austenite also appears in the form of thin films trapped in between bainitic ferrite plates (Fig. 7).

At lower austempering temperature (300ºC), the sheaves of bainite are finer because the driving force for transformation is higher as is the strength of the austenite. It is observed from the micrographs that blocky regions of austenite are smaller at the lower austempering temperature. The carbon partitioning from bainite makes the untransformed austenite more stable and the austenite can be seen at the cell boundaries. It is important to bear in mind that in general if more bainite is formed, less austenite is available for retention because bainite formation consumes austenite. Moreover, there is inhomogeneous distribution of carbon in the residual austenite after transformation to bainite. The austenite is enriched to a greater extent in the immediate vicinity to bainite platelets or in the region trapped between the platelets, while other region contains relatively poor carbon.

Coarse carbides were not observed but it seems from the micrographs that more fine dispersed particles of carbides can be seen inside sheaves of bainite (Figs. 6 and 7, arrowed).
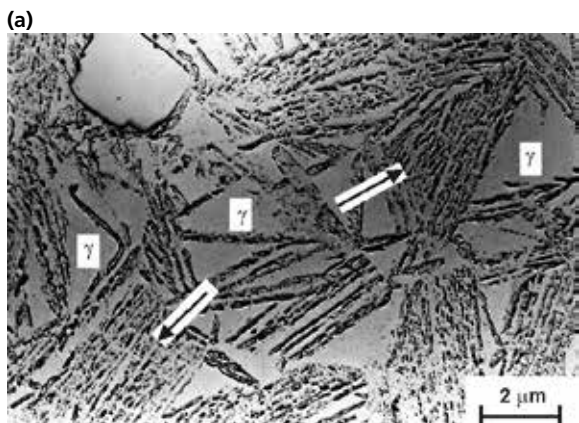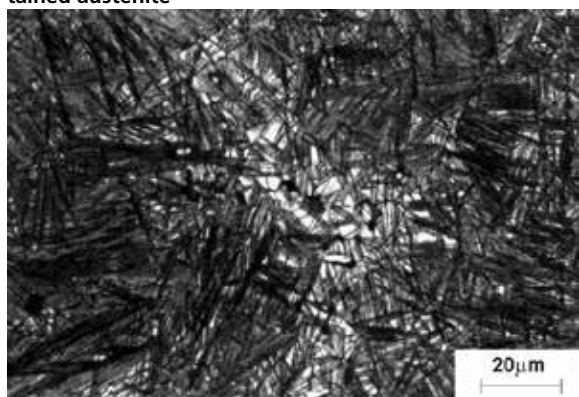
Fig. 6

(a)
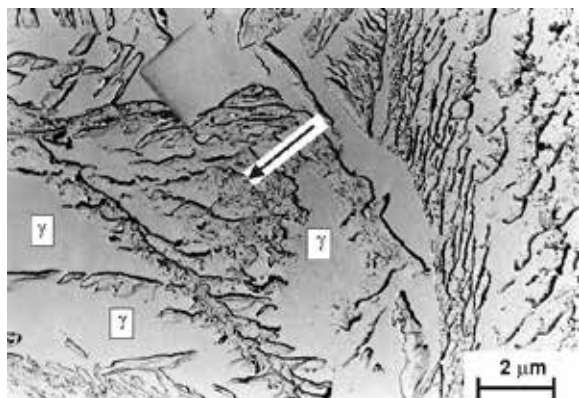
(b)

Fig. 6. Microstructure of ADI taken from sample austenitised at 950ºC and austempered at 400ºC for 120 min., a) optical micrograph, etched with 2% nital, b) carbon replica. This replica reveals the presence of carbides inside of bainite (arrowed) and shows large pools of blocky retained austenite

(a)

(b)

Fig. 7. Microstructure of ADI austenitised at 950ºC and austempered at 300ºC for 120 min. a) optical micrograph, etched with 2% nital, b) carbon replica. The carbon replica reveals the morphology of bainite which consists of fine plates of ferrite growing in clusters (arrowed) known as sheaves

3.3. Decarburisation of bainitic ferrite laths

The time required to decarburise a supersaturated bainitic ferrite lath of thickness w_α is given by[10,13]:

$$t_d = \frac{w_\alpha^2 \pi (\bar{x} - x^{\alpha\gamma})^2}{16 \overline{D}(x^{\gamma\alpha} - \bar{x})} \qquad (5)$$

where: $\bar{x}$ is the average carbon concentration in the alloy, $\overline{D}$

is weighted average diffusivity of carbon in austenite, $x^{\alpha\gamma}$ and $x^{\gamma\alpha}$ are the carbon concentrations in ferrite and austenite respectively, when the two phases are in paraequilibrium.

The good approximation of the dependent diffusivity of carbon in austenite can be a weighted average diffusivity $\overline{D}$.[15] Taking into account carbon concentration gradients it has been demonstrated that for most purposes a weighted average diffusivity $\overline{D}$ can adequately represent the effective diffusivity of carbon.[15-17] Weighted average diffusivity $\overline{D}$ is calculated by considering the carbon concentration profile in front of the moving ferrite interface as given by the following equation:

$$\overline{D} = \int_{\bar{x}}^{x^{\gamma\alpha}} \frac{D dx}{(x^{\gamma\alpha} - \bar{x})} \qquad (6)$$

The diffusion coefficient of carbon in austenite, $D\{x\}$, is very sensitive to the carbon concentration and this has to be taken into account in treating the large concentration gradients that develop in the austenite. It is clearly necessary to know $D\{x\}$ at least over a range, $\bar{x} \rightarrow x^{\gamma\alpha}$ although experimental determinations of $D\{x\}$ do not extent beyond x = 0.06. The value of **D** was calculated as discussed in Ref. [11]. The calculated diffusion coefficients of carbon sharply decreases with temperature (Table 2).

Table 2. The calculated diffusion coefficients of carbon in austenite $D\{x\}$ and a weighted average diffusivity $\overline{D}$ after austenitisation at 950 and 830ºC and austempering at 400, 350, 300 and 250ºC.

T_i, ºC	D [m²/s]	$\overline{D}$ [m²/s]
Austenitisation temperature, $T\gamma$ = 950ºC		
400	0.3574 x 10⁻¹⁵	0.1672 x 10⁻¹⁴
350	0.4688 x 10⁻¹⁶	0.5013 x 10⁻¹⁵
300	0.4328 x 10⁻¹⁷	*
250	0.2544 x 10⁻¹⁸	*
Austenitisation temperature, $T\gamma$ = 830ºC		
400	0.2088 x 10⁻¹⁵	0.1427 x 10⁻¹⁴
350	0.2714 x 10⁻¹⁶	0.4287 x 10⁻¹⁵
300	0.2482 x 10⁻¹⁷	*
250	0.1445 x 10⁻¹⁸	*

* Diffusion calculation outside of permitted range. Siller-McLellan model fails at high carbon concentrations evaluate $\overline{D}$.

The problem therefore becomes a calculation of the sum of the decarburisation times of all bainite laths that are existing on the coordinate connecting the nearest graphite nodules.

Figure 8 shows a schematic of eutectic cell that contains graphite nodules and packets of bainite with different thickness of ferrite laths.
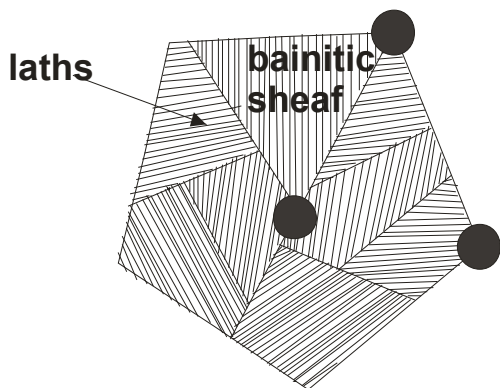
Fig. 8.
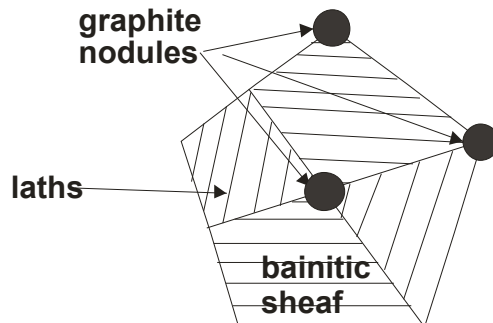
Fig. 8. Schematic of eutectic cell with different thickness of bainitic ferrite laths

The time needed to decarburise the ferrite matrix, t_{dz}, between the adjacent nodules of graphite:

$$t_{dz} = n_i \, t_{di} \qquad (7)$$

where n_i is the number of bainitic ferrite laths and t_{di} is the time required to decarburise individual supersaturated bainitic ferrite laths of specific thickness $w_{\alpha i}$.

Because of the inhomogeneous distribution of carbon and other solutes in the matrix after transformation to bainite the retained austenite is enriched to a greater extent in the immediate vicinity to bainite platelets or in the region trapped between the platelets and in the eutectic cell boundary (Fig. 9) while other regions contain relatively poor carbon.[9] The above effect can be exaggerated in ADI, since cast iron is usually extremely segregated. Martensite is usually found to be in the cell boundary which solidified last. It indicates that the austenite in cell boundary is less enriched with carbon, and therefore is thermally unstable.
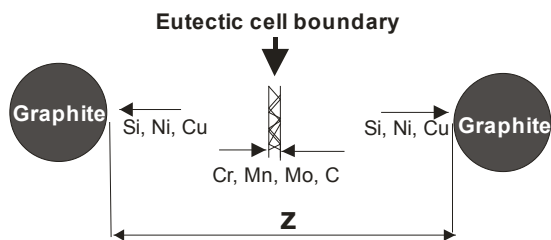
Fig. 9.

Fig. 9. Schematic of the direction of solute segregation between the adjacent graphite nodules

The calculated times of partitioning are shown in Fig. 10 and 11 for thickness of bainitic ferrite phase equal 50 μm but consisted of laths with different thickness: for $w_{\alpha i}$ = 500×0.1 μm; 250×0.2 μm; 100×0.5 μm; 50×1.0 μm; 5×10 μm and 50 μm after austenitisation and austempering at 400 and 350°C.

For investigated ductile cast iron ADI calculations of decarburisation times show that the decarburisation time t_d is a function of α phase width and increases with decreasing austempering temperature because the diffusion coefficient of carbon also decreases with temperature (Table 2).
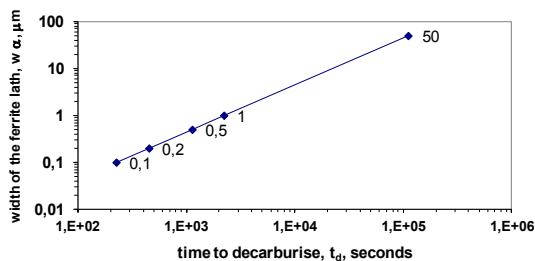
Fig. 10.

Fig. 10. The calculated decarburisation times for a given width of ferrite phase of 50 μm in investigated ADI consisted of laths with thickness: 500×0.1 μm; 250×0.2 μm; 100×0.5 μm; 50×1.0 μm; 5×10μm and 50 μm after austenitisation at 950oC

Fig. 11. The calculated decarburisation times td for a given width of ferrite phase in investigated ADI after austenitisation at 950 and 830oC and austempering at 400 and 350oC. The realationship (5) has been used for calculations.
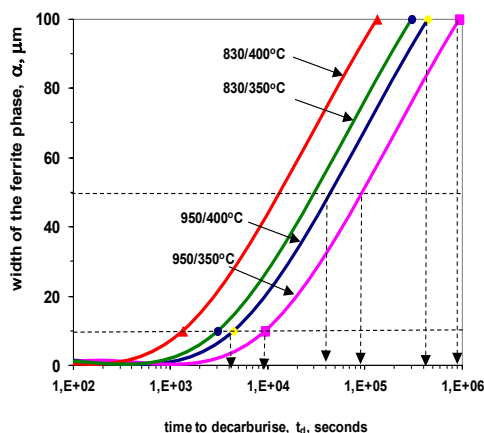
3.4. Carbon diffusion distances

The average carbon diffusion distances also depend on the mean spacing among the graphite nodules. Furthermore, it is generally observed that the width of ferrite laths is highly diverse. This reflect the possibility that cementite can precipitate in thicker bainite laths (when t_d is a long period of time) and in thinner laths has not during isothermal transformation. It is also consistent with the fact that upper and lower bainite often form at the same temperature in a given steel or ductile iron.[18,19] Thus, the calculated average carbon diffusion distances over specific periods of time (100, 1000 and 10000 s) are shown in Table 3.

Table 3. The calculated average carbon diffusion distances, z after 100, 1000 and 10000 seconds during austempering at 400 and 350oC after austenitisation at 950 and 830oC

Austempering temperature, T_i, oC	Carbon diffusion distances $z = 2\sqrt{Dt}$, m					
	Austenitisation temperature Tγ, oC					
	950			830		
	Austempering time, t, seconds					
	10^2	10^3	10^4	10^2	10^3	10^4
400	8.178×10⁻⁷	25.861×10⁻⁷	81.78×10⁻⁷	7.555×10⁻⁷	23.891×10⁻⁷	75.551×10⁻⁷
350	44.779×10⁻⁸	141.605×10⁻⁸	447.794×10⁻⁸	41.410×10⁻⁸	130.950×10⁻⁸	414.101×10⁻⁸

The calculated carbon diffusion distances in austenite in Table 3 illustrate that the estimated time is not capable of decarburising the ferrite laths during the period of austempering. Moreover, analytical calculations of the time required for the diffusion of carbon out of supersaturated laths of ferrite into the retained austenite also indicate that there is a necessity of carbides precipitation from ferrite. In the light of presented results it seems that using expression ausferrite transformation in the context of ductile cast iron is not justified and proper term is bainite transformation.

4. CONCLUSIONS

The paper presents an investigation of the carbon partitioning during bainitic reaction in ADI. The following conclusions were reached:

The bainite transformation in ductile cast iron is essentially identical to that in steel. In ductile iron, it has been demonstrated that the carbon concentration of the residual austenite reaches the critical value represented by the T_0 curve will render the displacive bainite reaction to cease. Therefore the carbon concentration of austenite can be estimated by the thermodynamics principles described here. Since cast iron is extremely segregated, x_γ determined by X-ray diffraction is richer than that corresponds to the T_0 curve in ADI

Analytical calculations of the time required for the diffusion of carbon out of supersaturated laths of ferrite into the retained austenite, carbon diffusion distances in austenite and measured extend of bainitic transformation indicate that there is a necessity of carbides precipitation from ferrite or austenite.

Precipitation of cementite leads to an increase of volume fraction of bainitic ferrite. Carbides locally reduce the carbon content of the parent austenite and increase the driving force for further ferrite growth.

A consequence of the precipitation of cementite from ferrite or/and austenite during austempering is that the growth of bainitic ferrite can continue to larger extent and that the resulting microstructure is not a pure ausferrite but is a mixture of bainitic ferrite, retained austenite and carbides.

REFERENCES

1. L.C. Chang: 'Carbon content of austenite in austempered ductile iron', Scripta Materialia, 1998, **39**, 35-38.
2. S. Pietrowski: 'Nodular cast iron of bainitic ferrite structure with austenite or bainitic structure', Archives of Materials Science, 1997, **18**, 253-273.
3. Z. Ławrynowicz and S. Dymski: 'Mechanism of bainite transformation in ductile iron ADI', Archives of Foundry Engineering, PAN, 2006, Vol.6, 171-176.
4. M.A. Yescas, H.K.D.H. Bhadeshia, D.J. Mac Kay: 'Estimation of the amount of retained austenite in austempered ductile irons using neural networks', Materials Science and Engineering, 2001, **A311**, 162-173.
5. Z. Ławrynowicz and S. Dymski: 'Application of the mechanism of bainite transformation to modelling of processing window in ductile iron ADI', Archives of Foundry Engineering, PAN, 2006, Vol.6, 177-182.
6. H.K.D.H. Bhadeshia: 'A Rationalisation of Shear Transformation in Steels', Acta Metallurgica, 1981, **29,** 1117-1130.
7. R.B. McLellan, W.W. Dunn: J. Phys. Chem. Solids., 1969, Vol.30, 2631.
8. H.K.D.H. Bhadeshia: 'Bainite: Overall Transformation Kinetics', Journal de Phys., 1982, Vol. 43, C4, 443-447.
9. Z. Ławrynowicz: 'Carbon Partitioning During Bainite Transformation in Low Alloy Steels, Materials Science and Technology, 2002, vol.18, 1322-1324.
10. H.K.D.H. Bhadeshia: 'Bainite in Steels', Institute of Materials, 1-458, 1992, London.
11. H.K.D.H. Bhadeshia: 'Diffusion of carbon in austenite', Metal Science, 1981, Vol.15, 477-479.
12. Z. Ławrynowicz and A. Barbacki: 'The mechanism of bainite transformation in Fe-Cr-Mn-Si-C steel', Proc. of the Scientific Con. AMTECH'95, Rousse, Bułgaria, 19-21 April 1995, 1-8.
13. H.K.D.H. Bhadeshia and J.W. Christian: 'Bainite in Steels', Metallurgical Transactions A, 1990, **21A**, 767-797.
14. M. Takahashi and H.K.D.H. Bhadeshia: 'A Model for the Microstructure of Some Advanced Bainitic Steels', Materials Transaction, JIM, 1991, Vol.32, 689-696.
15. R.H. Siller, R.B. McLelan: 'The Application of First Order Mixing Statistics to the Variation of the Diffusivity of Carbon in Austenite', Metallurgical Transactions, 1970, Vol.1, 985-988.
16. Z. Ławrynowicz: 'Affect of cementite precipitation on the extend of bainite reaction in ADI', Journal of Polish CIMAC, 2013, vol. 8, 31-36.
17. Z. Ławrynowicz: 'Bainitic transformation: estimation of carbon diffusivity in austenite on the basis of measured austenite film thickness', Zeszyty Naukowe ATR nr 216, 1998, Mechanika 43, 289-297. (in Polish).
18. M. Takahashi and H.K.D.H. Bhadeshia: 'Model for transition from upper to lower bainite', Material Science and Technology, 1990, **6**, 592-603.
19. Ławrynowicz Z.: "Transition from upper to lower bainite in Fe-Cr-C steel', Materials Science and Technology, 2004, **20,** 1447-1454.